Regeneration of Sooty Surface Using Nanosecond Pulsed Dielectric Barrier Discharge

Noureddine Zouzou, Arthur Claude Aba'a Ndong, Éric Moreau

▶ **To cite this version:**

Noureddine Zouzou, Arthur Claude Aba'a Ndong, Éric Moreau. Regeneration of Sooty Surface Using Nanosecond Pulsed Dielectric Barrier Discharge. IEEE Transactions on Industry Applications, 2017, 53 (4), pp.3982-3988. ⟨10.1109/TIA.2017.2682168⟩. ⟨hal-04484593⟩

HAL Id: hal-04484593

https://hal.science/hal-04484593v1

Submitted on 19 May 2025

HAL is a multi-disciplinary open access archive for the deposit and dissemination of scientific research documents, whether they are published or not. The documents may come from teaching and research institutions in France or abroad, or from public or private research centers.

L'archive ouverte pluridisciplinaire **HAL**, est destinée au dépôt et à la diffusion de documents scientifiques de niveau recherche, publiés ou non, émanant des établissements d'enseignement et de recherche français ou étrangers, des laboratoires publics ou privés.

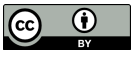

Distributed under a Creative Commons CC BY 4.0 - Attribution - International License

Regeneration of Sooty Surface using Nanosecond Pulsed Dielectric Barrier Discharge

Noureddine Zouzou, Arthur Claude Aba'a Ndong, Eric Moreau
Institut Pprime, UPR 3346, CNRS – Université de Poitiers – ISAE-ENSMA
SP2MI, Téléport 2, Bd. Marie & Pierre Curie, BP. 30179
F86962, Futuroscope, France
noureddine.zouzou@univ-poitiers.fr

***Abstract* -- In this paper, the regeneration of sooty surface by using nanosecond pulsed surface dielectric barrier discharge type reactor is investigated experimentally. The goal is to characterize the regeneration process as a function of the applied voltage magnitude and pulse polarity. The reactor is composed of two electrodes separated by a dielectric and arranged asymmetrically. The power supply system provides high voltage pulses with the following characteristics: voltage up to ±10 kV, rise and decay times less than 50 ns and a frequency of 2 kHz. The main results show that the regeneration performance increases with the applied voltage magnitude and the duration of treatment. Furthermore, depending on the polarity and the magnitude of the applied voltage pulse, the cleaned surface area can be either more uniform along the active electrode (negative pulses), either extended on the dielectric surface (positive pulses). The regeneration mechanism remains not very well understood, but it seems that the soot particle size is reduced mainly due to the interaction with ozone molecules and oxygen radicals generated by the discharge.**

***Index Terms*-- Diesel particles, Surface regeneration, Surface Dielectric Barrier Discharge, Nanosecond Pulsed High Voltage, Non-Thermal Plasma, Electrostatic Precipitation.**

I. INTRODUCTION

Combustion systems such as diesel engines are responsible of soot particles emission in the atmosphere, which contributes to the deterioration of air quality [1], [2]. The adverse effects of fine particles did not concern only the open atmosphere; the confined spaces could contain much more particles in certain situations [3], [4]. In traffic jams or in tunnels for instance, the passengers in a vehicle are strongly exposed to the external pollution.

In order to respect the future legislative limits protecting the human health, a combination of engine modifications and after-treatment technologies are extensively investigated in the past years [5-7]. In particular, the electrostatic precipitation is considered as the most promising technology for the collection of ultrafine particles emitted from diesel engines [8-12]. However, it should be cleaned or regenerated periodically to maintain its performance. Therefore, the collected diesel particles must be incinerated or swept from the surface after agglomeration in order to be collected and processed by another technology, such as in diesel particulate filter [13].

The possibility of sooty surface regeneration by using AC surface dielectric barrier discharge (SDBD) has been explored in the past few years [14], [15]. In fact, this discharge could resolve this issue through the action of: (1) the electric wind generated near the wall where the particles are deposited; (2) the Coulomb force acting on the electrically charged particles; and/or (3) the ozone molecules and oxygen radicals allowing the oxidation of soot.

In this paper, diesel particle regeneration by using nanosecond pulsed SDBD type reactor is investigated experimentally. The main objective of this study is to characterize the regeneration process as a function of the applied voltage magnitude and pulse polarity. In fact, nanosecond pulsed voltage has two main advantages compared to AC voltage in the field of surface regeneration using a SDBD: the ability to inject very high energy in a short time, and the control of the plasma morphology by changing the pulse polarity.

In the first part of the paper, the experimental setup is described. Then, results concerning discharge characteristics and particle regeneration are discussed. Finally, conclusions are summarized.

II. EXPERIMENTAL SETUP

A. *Reactor design*

The SDBD reactor used for particle regeneration is composed of two electrodes (aluminum foils, 70 µm thickness) separated by a dielectric barrier (Pyrex, 1 mm thickness) and arranged asymmetrically in edge-to-edge manner (Fig. 1). The so-called HV or active electrode (10 mm width) is supplied with a nanosecond pulsed high voltage. The grounded electrode (25 mm width) is placed on the other side of the dielectric and encapsulated inside an epoxy resin. The spanwise length of the electrodes is about 100 mm.

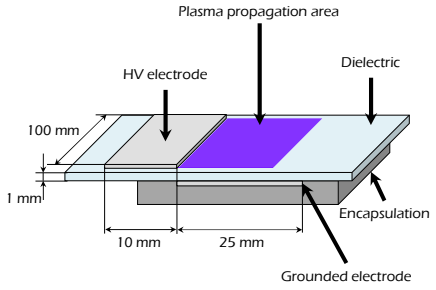

Fig. 1. Schematic illustration of the SDBD reactor.

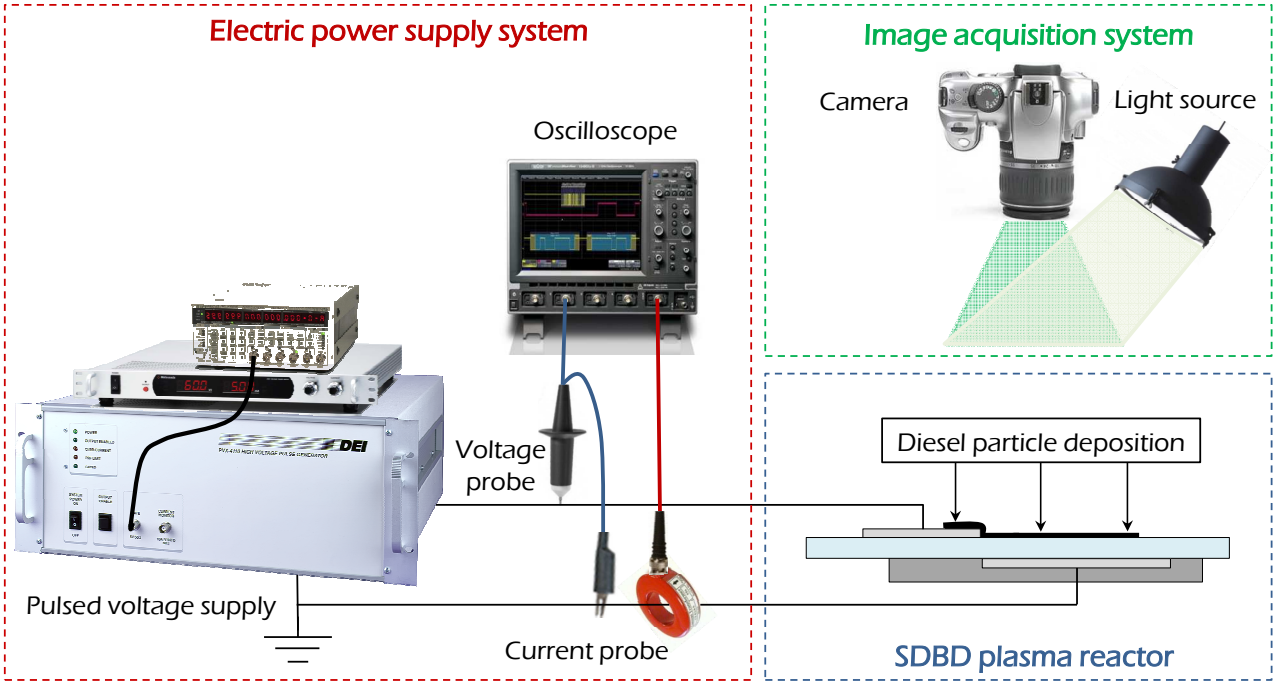

Fig. 2. Schematic illustration of the experimental setup.

B. *Experimental setup*

The experimental setup used for surface regeneration is illustrated schematically in Fig. 2. It consists of an electric power supply system, an image acquisition system and the SDBD plasma reactor.

The power supply system is composed with an HV solid-state pulser (DEI, model PVX-4110, ± 10 kV, ± 30 A_{peak}), a DC power supply (Matsusada, model 10P30, ± 10 kV, ± 30 mA) and a digital pulse generator (Stanford, model DG645). The system can provide nanosecond pulsed high voltage with the following characteristics: high voltage magnitude up to ±10 kV, rise and decay times less than 50 ns and frequency up to 10 kHz.

The current and voltage waveforms are recorded using a digital oscilloscope (Lecroy, model WaveSurfer 424, 200 MHz bandwidth) connected to dedicated probes. The current probe is a fast current transformer (Bergoz, model CT-D1.0, 500 MHz bandwidth). The voltage across the reactor is measured with a high voltage probe (Lecroy, model PPE20kV, 100 MHz bandwidth).

Smoke coming from diesel burning is used to deposit a thin layer of soot where the surface discharge will occur (near the HV electrode). Then, the regeneration performance is studied by analyzing the photographs of the contaminated surface as a function of electrical parameters. The images are captured using a CMOS camera (Canon, model EOS 300D, 8 bits) coupled with a macro lens (Canon, EF 100 mm f/2.8, USM). The camera is set in manual mode with a delay of 10 s, an exposure time of 50 ms and a resolution of 3072 × 2048 pixels. The size of the visualization field is about 64 × 42.6 mm^2.

All the regeneration experiments are carried out at atmospheric pressure and room temperature.

III. Results and Discussion

In following sections, the typical current waveform, the power consumption of the reactor, the plasma morphology and the regeneration performance are discussed.

A. *Electrical characteristics*

Fig. 3 shows typical waveforms of the measured current with and without the presence of particles in the case of negative high voltage pulses. The waveforms are acquired 30 s after the application of the voltage. The signature of two well resolved peaks is observed during each transition of the applied voltage (from 0 to -10 kV then from -10 to 0 kV). The first current peak, related to the capacitive effect, is not sensitive to the presence of particles on the dielectric surface. The second peak is due to the occurrence of the discharge. Its magnitude becomes higher with the presence of particles, due to the enhancement of the surface electrical conductivity.

The evolution of electric power consumption with the treatment duration is shown in Fig. 4. The mean power is calculated by integrating the product of the voltage and the current (instantaneous power) over a period. To confirm the trend, we calculated the averaged value over 100 pulses for each point using the oscilloscope software. The standard deviation values are also indicated in Fig. 4.

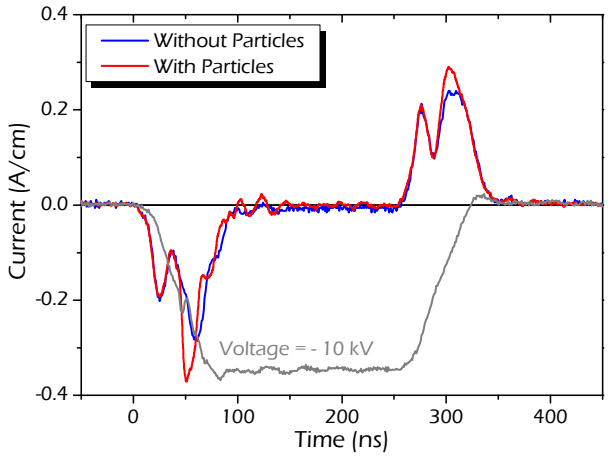

Fig. 3. Time evolution of the current per unit length of the electrodes after 30 s of treatment. Conditions: voltage magnitude = -10 kV, frequency = 2 kHz, pulse width = 250 ns.

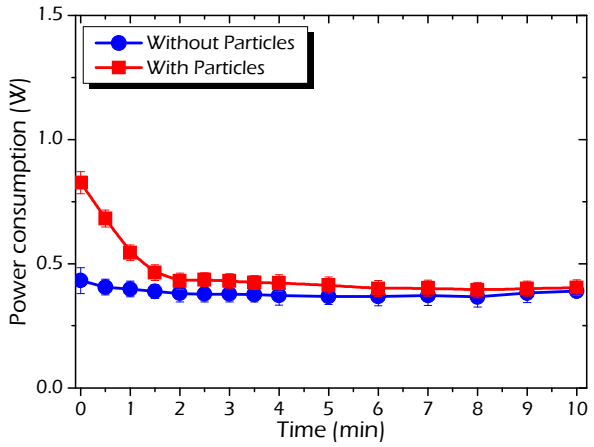

Fig. 4. Influence of the presence of particles on power consumption. Conditions: voltage = -10 kV, frequency = 2 kHz, pulse width = 250 ns.

As expected, the power is higher with the presence of particles. This is explained by the fact that the soot layer makes the surface of the dielectric more conductive. Thus, the electric field near HV electrode edge still at higher level because the deposited charges migrate far from the active area. After 10 min of treatment, the electric power becomes equal to that measured in the case of a clean surface. Therefore, the power measurement could be considered as a good indicator of surface treatment progress.

B. Morphology of plasma

In this section, we will present a diagnosis of the plasma layer for both positive and negative polarities. The top-view images are recorded using an intensified charge coupled device (iCCD) camera (Princeton Instruments, model Pi-Max2/Gen2) with 1024×1024 pixels matrix. The camera is placed in front of the plasma sheet. Even if the camera is able to acquire images with an opening gate width of about 2 ns, we choose to present only images with long opening gate width (from t = 0 to 200 ns).

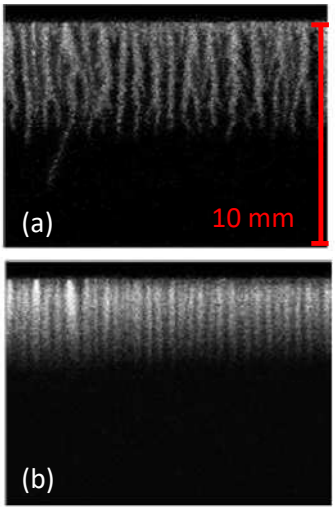

Fig. 5. Top view of the plasma layer corresponding to (A) positive rising voltage, and (B) negative falling voltage. Conditions: voltage = ± 10 kV, frequency = 0.5 kHz, pulse width = 250 ns, opening gate width = 200 ns, the active electrode located in the top side of the images.

Fig. 5 illustrates the plasma layer for both polarities without the presence of particles. In the case positive rising voltage (transition from 0 to 10 kV), the plasma layer is composed of many filaments distributed along the HV electrode, and the discharge operates in a streamer-like regime. The channels of streamers are straight, well-distributed and distinct.

For the negative falling voltage (transition from 0 to -10 kV), the plasma layer in composed of several ionization regions, each one starting from a corona spot in contact with the active electrode and expanding in the direction of the grounded electrode in a plume shape. The plasma is quite diffuse and homogeneous along the active electrode.

This result is similar to the one obtained using polyamide as a dielectric barrier instead of glass, under similar electrical conditions [16], [17].

C. Performance index

Fig. 6 shows the typical top view photographs taken before and after regeneration using negative voltage pulses. A treated area is clearly observed on the dielectric surface close to the HV electrode.

To evaluate the regeneration performance associated to each pixel of the greyscale image, a performance index (I_p) using the following equation is used:

$$I_p(\%) = \frac{C_2 - C_1}{C_2 + C_1} \times 100 \qquad (1)$$

where C_1 and C_2 are the greyscale levels of the images taken before and after treatment, respectively. The grey levels range from 0 (black) to 255 (white), with 256 possible values for each pixel (8 bits).

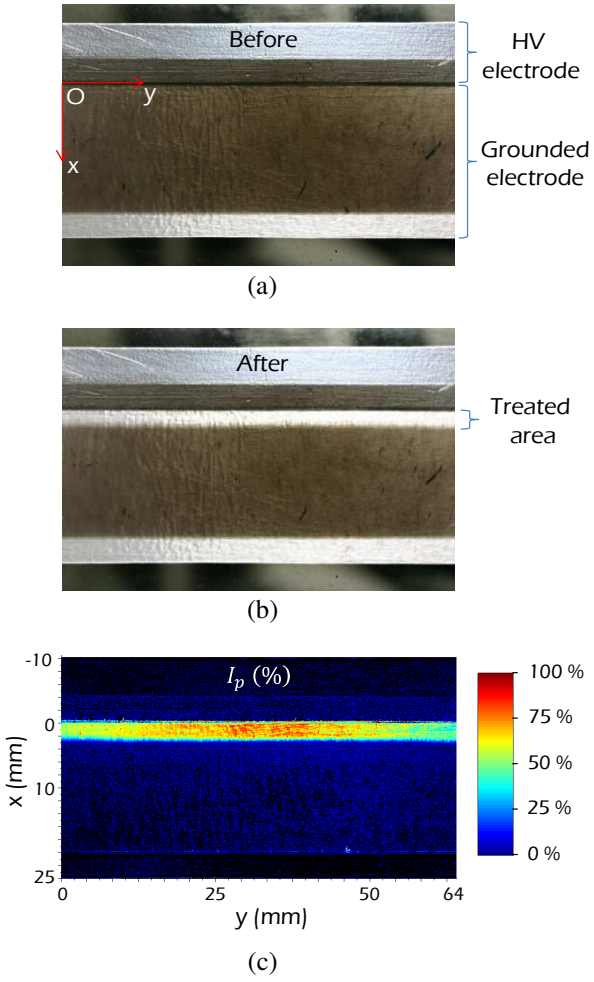

Fig. 6. Evaluation of the regeneration performance: (a) the reactor photograph taken before treatment, (b) the reactor photograph after treatment, and (c) the associated performance index map. Conditions: voltage magnitude = -10 kV, frequency = 2 kHz, pulse width = 250 ns, regeneration duration = 4 min.

One can identify several specific cases:

- $C_2 \approx C_1$: the regeneration did not occur or has a very weak effect on the soot layer. So, the performance index is close to zero ($I_p \approx 0$ %);

- $C_2 >> C_1$: the regeneration process is very efficient. The performance index is therefore at the highest level ($I_p \approx 100$ %). However, in practice, I_p is never equal to 100% because this is the case only if $C_1 = 0$, corresponding to a fully black surface. Then a perfectly cleaned surface can correspond to I_p < 100%, depending on the value of C_1;

- $C_2 < C_1$: the particle density is higher after the regeneration process. In this case, the performance index is negative and can be interpreted by a migration of particles on the dielectric surface.

A typical example of the performance index calculation on each pixel of the viewing area is given in Fig. 6c. For instance, the performance index values are ranged from 50 % to 75 % in the vicinity of the HV electrode.

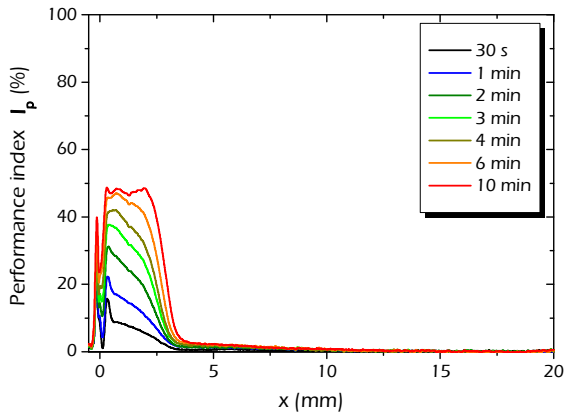

Fig. 7. Performance index profiles along x-direction for different treatment duration. Conditions: voltage = -10 kV, frequency =2 kHz, pulse width =250ns.

D. *Effect of treatment duration*

In this section, the evolution of the regeneration process as a function of the treatment duration is investigated in the case of negative high voltage pulses. In this paper, only averaged profiles of the performance index along x-direction are plotted for different treatment durations as illustrated in Fig. 7. The results show that the performance index increases gradually with time near the HV electrode where the discharge takes place ($0 \leq x \leq 3$ mm). The surface discharge seems to have a weak effect on the soot layer after about 6 min of treatment. The maximum value of I_p did not exceed 50 % within the experimental conditions considered in Fig. 7.

E. *Effect of voltage magnitude and pulse polarity*

In this section, surface regeneration process is examined by varying the high voltage magnitude for both negative and positive polarities.

Fig. 8 shows the typical top view photographs of the reactor after only 2 min of treatment because after 10 min, the surface is cleaned and one cannot observe correctly the voltage effect. In the case of negative pulses, the treated area has the shape of plumes channels connected to the HV electrode. The number of these channels increases continuously with voltage magnitude. For –10 kV, the regenerated zone is more or less uniform along the HV electrode. In the case of positive pulses, the treated area is completely different compared to the negative case. It extends much more in x-direction (up to x = 13 mm) and becomes non-uniform with increasing the applied voltage. For instance, an apparent increase in particle density is observed in the area 2.5 mm $\leq$ x $\leq$ 5 mm for voltage magnitudes greater than +8 kV.

Consequently, the footprint of the discharge on the soot deposit is very similar to the shape of the plasma layer on a clean surface shown in Fig. 5.

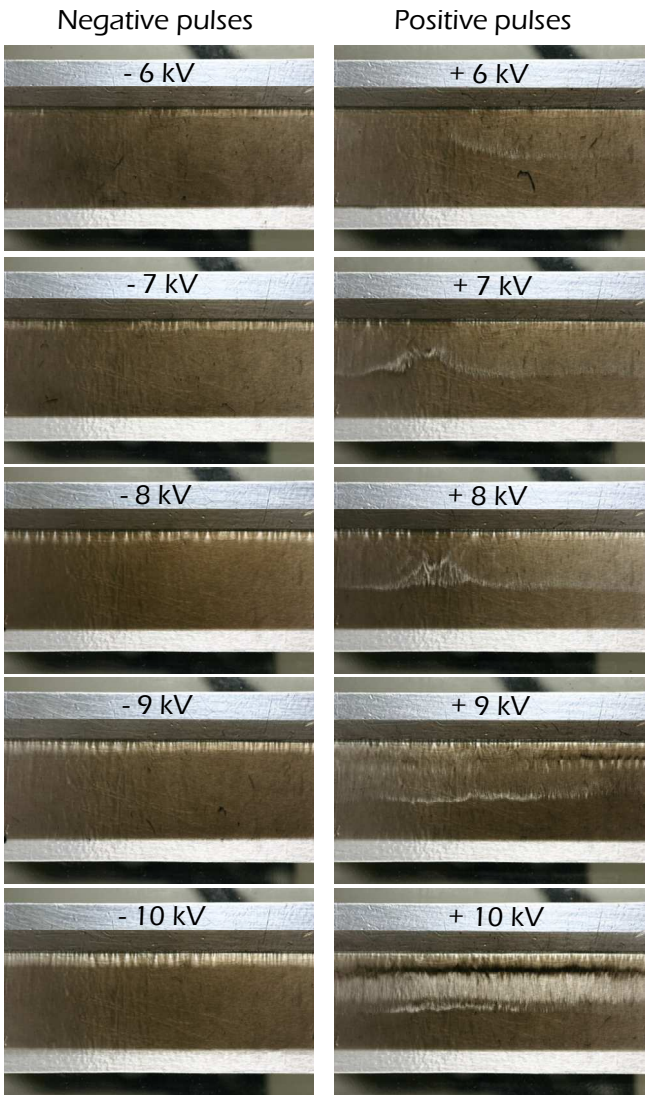

Fig. 8. Evolution of reactor photographs as a function of the applied voltage magnitude. Conditions: frequency = 2 kHz, pulse width = 250 ns, treatment duration = 2 min.

Fig. 9 illustrates the average profiles of the performance index in x-direction for both polarities. With increasing the applied voltage, the width of the treated area on the dielectric surface increases up to x = 3 mm for negative polarity and x = 13 mm for positive one. Moreover, the performance index maximum increases gradually with the applied voltage. For positive voltage magnitude = + 10 kV, the performance index reaches 40 % for 5 mm ≤ x ≤ 10 mm and becomes negative (about -50 %) in the zone 2.5 mm ≤ x ≤ 5 mm. This result could be explained by a phenomenon of particles migration, due to the strong Coulomb force acting on positively charged particles during the transition of the applied voltage from +10 to 0 kV.

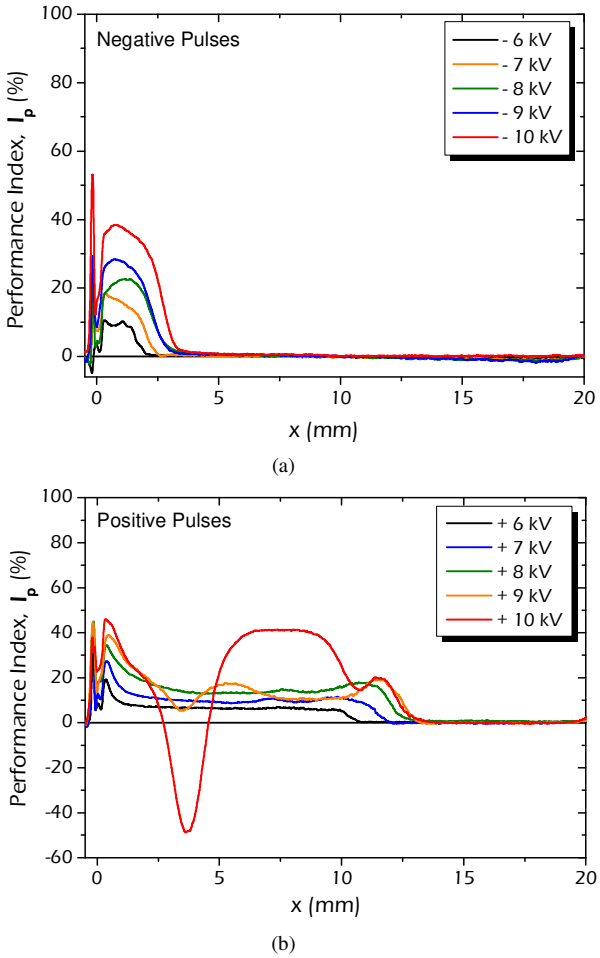

Fig. 9. Performance index profiles along x-direction for (a) negative and (b) positive pulses. Conditions: frequency = 2 kHz, pulse width = 250 ns, treatment duration = 2 min.

F. Regeneration mechanism

The mean size of particles produced by the interaction between the discharge and the soot layer has been investigated using an electrical low pressure impactor (Dekati, model ELPI+, particle size from 0.006 to 10 µm).

Fig. 10 shows a typical example of particle size distribution of the diesel particles deposited on the dielectric surface prior the regeneration process. The results show that dominant particles are in the size range between 0.26 µm and 0.38 µm.

To measure the particles size produced by the regeneration process, the SDBD reactor is introduced in a test chamber (volume of 15 L) with a clean air flow rate of about 10 $L.min^{-1}$. Then, the size of particles produced by the regeneration process is measured at the outlet of the test chamber. Fig. 11 illustrates the average size distributions of the particles measured during the first minute of treatment with positive and negative high voltage pulses. The detected particles are in the size range between 0.054 µm and 0.094 µm. One can conclude that the regeneration process creates new particle population smaller to the one before treatment.

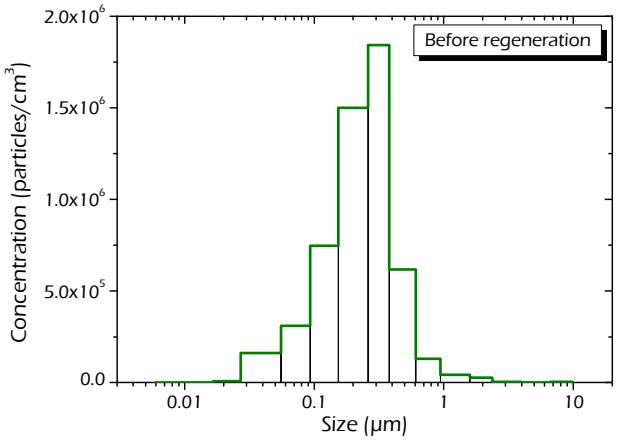

Fig. 10. Typical particle size distribution of the deposited diesel particles.

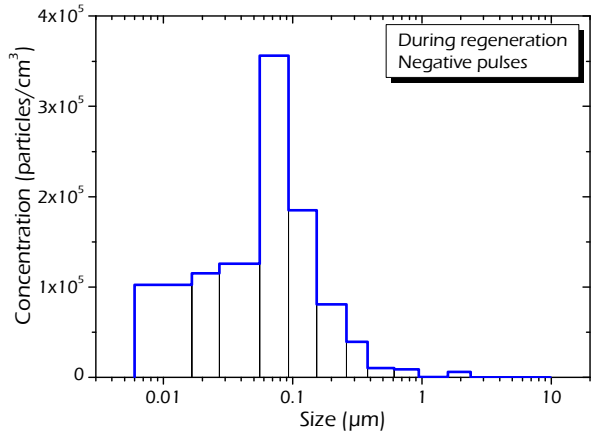

(a)

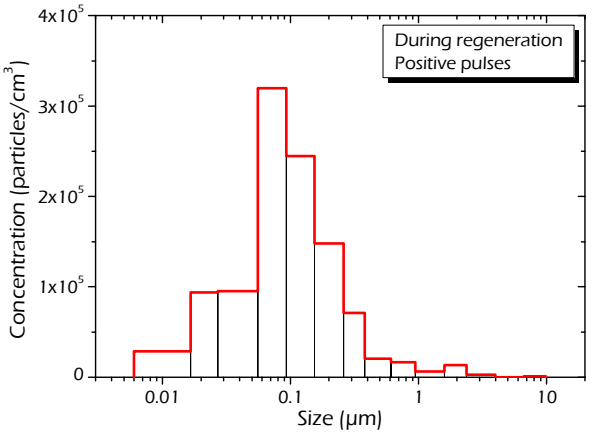

(b)

Fig. 11. Particle size distribution produced during the first minute of regeneration for (a) negative and (b) positive pulses. Conditions: voltage = ± 10 kV, frequency = 2 kHz, pulse width = 250 ns, flowrate = 10 L.min^{-1}.

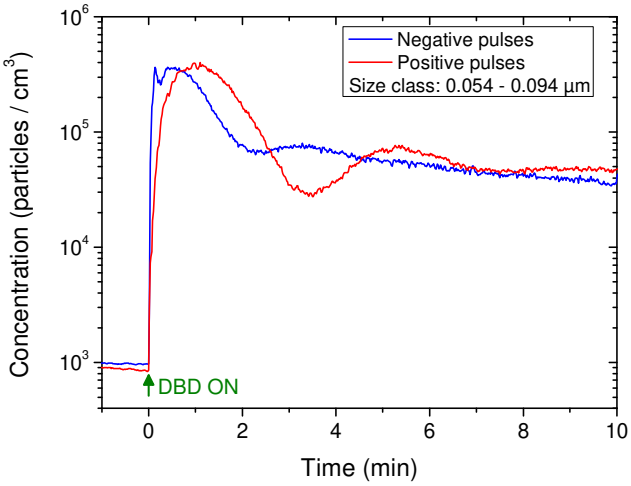

Fig. 12. Time evolution of particles concentration for particles size class 0.055 – 0.094 µm. Conditions: voltage = ± 10 kV, frequency = 2 kHz, pulse width = 250 ns, flowrate = 10 L.min^{-1}.

Fig. 12 shows a typical time evolution of particles concentration corresponding to size class 0.054 – 0.094 µm for both pulse polarities. The particle concentration in the gas that surrounds the SDBD reactor is about 10^3 particles / cm^3, which is similar to the typical indoor concentration. When the voltage is turned on, the particles concentration increases by more than two orders of magnitude. One can note that the maximum concentration value is reached more quickly in the case of negative polarity (after about 30 s). Then, the concentration decreases with time for both polarities but still higher than the typical indoor concentration.

Several papers reported the ability of volume DBD to oxidize soot particles even at low temperature, due to ozone molecules and oxygen radicals [18]-[21]. These active species are also produced with nanosecond pulsed surface DBD. Thus, some amount of the deposited particles could be partially oxidized into CO and CO_2, which explains the appearance of smaller particles.

IV. Conclusion

In this paper, the regeneration of sooty surface by using nanosecond pulsed surface dielectric barrier discharge type reactor have been investigated. The main results of this experimental study are as follows.

(1) The discharge current increases with the presence of particles, due to the enhancement of the surface conductivity.

(2) The power consumption decreases with the treatment duration until reaching the same power level of a clean reactor. It could be considered as a good indicator of surface treatment progress.

(3) Depending on the polarity of the applied voltage pulse, the cleaned surface area can be either more uniform along the

active electrode (case of negative pulses) either more extended on the dielectric surface (case of positive pulses). In fact, the treated area is very similar to the one of the surface plasma that develops at the dielectric wall in the case of clean reactor.

(4) The soot particle is reduced in size during the regeneration due to their interaction with the SDBD.

Obviously, these experiments were preliminary ones and we are well aware that further investigations are necessary to understand more clearly the effect of surface discharge on soot layer by using chemical analysis methods.

ACKNOWLEDGMENT

This research work has received funding from the AIRD-STDF joint innovative projects fund program (AAP STDF 3 AIRD 2013-2014) under the grant agreement N° 784592.

REFERENCES

[1] H. Burtscher, "Physical characterization of particulate emissions from diesel engines: a review," *J. Aerosol Sci.*, vol. 36, pp. 896-932, 2005.

[2] M. Matti Maricq, "Chemical characterization of particulate emissions from diesel engines: A review," *J. Aerosol Sci.*, vol. 38, no. 11, pp. 1079–1118, 2007.

[3] K. Oravisjärvi, M. Pietikäinen, J. Ruuskanen, and A. Rautio, A. Voutilainen, R. L. Keiski, "Effects of physical activity on the deposition of traffic-related particles into the human lungs in silico," *Sci. Total Environ.*, vol. 409, pp. 4511-4518, 2011.

[4] J. O. Anderson , J. G. Thundiyil, and A. Stolbach, "Clearing the Air: A Review of the Effects of Particulate Matter Air Pollution on Human Health," *J. Med. Toxicol.*, vol. 8, no. 2, pp. 166-175, 2012.

[5] D. Sonar , S. L. Soni, D. Sharma, A. Srivastava, and R. Goyal, "Performance and emission characteristics of a diesel engine with varying injection pressure and fuelled with raw mahua oil (preheated and blends) and mahua oil methyl ester," *Clean Technol. Environ. Policy*, vol. 17, no. 6, pp. 1499-1511, 2015.

[6] M. Babaie , T. Kishi, M. Arai, Y. Zama, T. Furuhata, Z. Ristovski, H. Rahimzadeh, and R. J. Brown, "Influence of non-thermal plasma after-treatment technology on diesel engine particulate matter composition and NOx concentration", Int. *J. Environ. Sci. Technol.*, vol. 13, no. 1, pp. 221-230, 2016.

[7] B. A. A. L. Van Setten, M. Makkee, and J. A. Moulijn, "Science and technology of catalytic diesel particulate filters", Catal. Rev., vol. 43, no. 4, pp. 489–564, 2001.

[8] S. Masuda, and J. D. Moon, "Electrostatic Precipitation of Carbon Soot from Diesel Engine Exhaust," *IEEE Trans. Ind. Appl.*, vol. IA-19, no. 6, pp. 1104 - 1111, 1983.

[9] P. Saiyasitpanich, T.C. Keener, S.-J. Khang, and M. Lu, "Removal of diesel particulate matter (DPM) in a tubular wet electrostatic precipitator", *J. Electrostat.*, vol. 65, no. 10–11, pp. 618–624, 2007

[10] T. Yamamoto, T. Mimura, N. Otsuka, Y. Ito, Y. Ehara, and A. Zukeran, "Diesel PM collection for marine and automobile emissions using EHD electrostatic precipitators", *IEEE Trans. Ind. Appl.*, vol. 46, pp (2010) 1606-1612, 2010.

[11] M. Takasaki, H. Kurita, T. Kubota, K. Takashima, M. Hayashi, and A. Mizuno, "Electrostatic precipitation of diesel PM at reduced gas temperature", *in Proc. of the 2015 IEEE Industry Applications Society Annual Meeting*, 18-22 October 2015, Dallas, Texas, USA.

[12] A. Sudrajad, and A. F. Yusof, "Review of Electrostatic Precipitator Device for Reduce of Diesel Engine Particulate Matter," *Energy Procedia*, vol. 68, pp. 370-380, 2015

[13] H. Hayashi, Y. Takasaki, K. Kawahara, K. Takashima, and A. Mizuno, "Electrostatic Charging and Precipitation of Diesel Soot," *IEEE Trans. Ind. Appl.*, vol. 47, no. 1, pp. 331-335, 2011.

[14] N. Zouzou, C. Agbangla, E. Moreau, and G. Touchard, "Diesel particle treatment using a Surface Dielectric Barrier Discharge," *IEEE Trans. Plasma Sci.*, vol. 36, no. 4, pp. 1354-1355, 2008.

[15] N. Zouzou, K. Takashima, A. Mizuno, and G. Touchard, *Generation and application of wide area plasma, Chapter 8 of Industrial plasma Technology: Application from Environmental to Energy Technologies*, Weinheim: Wiley-VCH, 2010.

[16] A. C. Aba'a Ndong, N. Zouzou, N. Benard, and E. Moreau, "Geometrical optimization of a surface DBD powered by a nanosecond pulsed high voltage," *J. Electrostat.*, vol. 71, no. 3, pp. 246-253, 2013.

[17] A. C. Aba'a Ndong, N. Zouzou, N. Benard, and E. Moreau, "Effect of the dielectric aging on the behavior of a surface nanosecond pulsed DBD," *IEEE Trans. Dielectr. Elect. Insul.*, vol. 20, no. 5, pp. 1554-1560, 2013.

[18] M. Okubo, T. Kuroki, Y. Miyairi, and T. Yamamoto, "Low-temperature soot incineration of diesel particulate filter using remote nonthermal plasma induced by a pulsed barrier discharge," *IEEE Trans. Ind. Appl.*, vol. 40, no. 6, pp. 1504 - 1512, 2004.

[19] J. Grundmann, S. Müller, and R.-J. Zahn, "Treatment of Soot by Dielectric Barrier Discharges and Ozone", *Plasma Chem. Plasma Process.*, vol. 25, no. 5, pp. 455-466, 2005.

[20] S. Yao, C. Fushimi, K. Madokoro, and K. Yamada, "Uneven Dielectric Barrier Discharge Reactors for Diesel Particulate Matter Removal," *Plasma Chem. Plasma Process.*, vol. 26, pp. 481-493, 2006.

[21] M. Okubo, T. Kuroki, K. Yoshida, and T. Yamamoto, "Single-Stage Simultaneous Reduction of Diesel Particulate and NOx Using Oxygen-Lean Nonthermal Plasma Application," *IEEE Trans. Ind. Appl.*, vol. 46, no. 6, pp. 2143 - 2150, 2010.